Single-Walled Carbon Nanotubes Alter Cytochrome *c* Electron Transfer and Modulate Mitochondrial Function

Xiaowei Ma,[†,⊥] Li-Hua Zhang,[†,‡,⊥] Li-Rong Wang,[†,⊥] Xue Xue,[†] Ji-Hong Sun,[‡,*] Yan Wu,[†] Guozhang Zou,[†] Xia Wu,[†,‡] Paul C. Wang,[§] Wayne G. Wamer,[∥] Jun-Jie Yin,[∥] Kaiyuan Zheng,[†] and Xing-Jie Liang[†,*]

[†]Laboratory of Nanomedicine and Nanosafety, Division of Nanomedicine and Nanobiology, National Center for Nanoscience and Technology, China, and CAS Key Laboratory for Biomedical Effects of Nanomaterials and Nanosafety, Chinese Academy of Sciences, Beijing 100190, China, [‡]Department of Chemistry & Chemical Engineering, College of Environment and Energy Engineering, Beijing University of Technology, Beijing 100124, China, [§]Molecular Imaging Laboratory, Department of Radiology, Howard University, Washington, D.C. 20060, United States, and [∥]Center for Food Safety and Applied Nutrition, Food and Drug Administration, College Park, Maryland 20740, United States. [⊥]These authors contributed equally to this work.

ABSTRACT Single-walled carbon nanotubes (SWCNTs) are broadly used for various biomedical applications such as drug delivery, *in vivo* imaging, and cancer photothermal therapy due to their unique physiochemical properties. However, once they enter the cells, the effects of SWCNTs on the intracellular organelles and macromolecules are not comprehensively understood. Cytochrome *c* (Cyt *c*), as a key component of the electron transport chain in mitochondria, plays an essential role in cellular energy consumption, growth, and differentiation. In this study, we found the mitochondrial membrane potential and mitochondrial oxygen uptake were greatly decreased in human epithelial KB cells treated with SWCNTs, which accompanies the reduction of Cyt *c*. SWCNTs deoxidized Cyt *c* in a pH-dependent manner, as evidenced by the appearance of a 550 nm characteristic absorption peak, the intensity of which increased as the pH increased. Circular dichroism measurement confirmed the pH-dependent conformational change, which facilitated closer association of SWCNTs with the heme pocket of Cyt *c* and thus expedited the reduction of Cyt *c*. The electron transfer of Cyt *c* is also disturbed by SWCNTs, as measured with electron spin resonance spectroscopy. In conclusion, the redox activity of Cyt *c* was affected by SWCNTs treatment due to attenuated electron transfer and conformational change of Cyt *c*, which consequently changed mitochondrial respiration of SWCNTs-treated cells. This work is significant to SWCNTs research because it provides a novel understanding of SWCNTs' disruption of mitochondria function and has important implications for biomedical applications of SWCNTs.

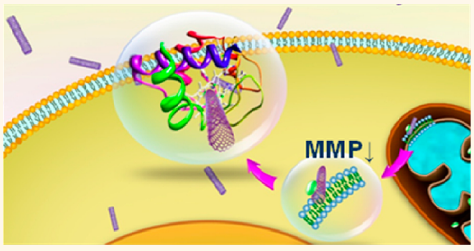

KEYWORDS: single-walled carbon nanotubes · carboxy · cytochrome *c* · electron transfer · mitochondrial function · redox activity

Carbon nanomaterials with tunable surface properties and good biocompatibility have great potential for biological and medical applications.[1,2] As a unique quasi one-dimensional material, SWCNTs have been explored as novel delivery vehicles for drugs, peptides, proteins, plasmid DNA, and small interfering RNA.[3] The interactions between biological macromolecules and carbon nanomaterials have been reported to cause changes in the structure and function of proteins.[2,4−10] When the functionalized carbon nanotubes recognize and bind to the catalytic site of α-chymotrypsin, its enzymatic activity was inhibited completely.[6] Karajanagi *et al.* demonstrated that activities of α-chymotrypsin (CT) and soybean peroxidase (SBP) were differently affected by their interaction with SWCNTs. It was found that SBP retained its native three-dimensional conformation and up to 30% of its native activity after interaction with SWCNTs. In contrast, α-CT unfolded on the SWCNT surface and retained only 1% of its original activity.[5] Proteins can bind with SWCNTs through covalent or noncovalent interactions due to their large surface areas. SWCNTs tend to strongly bind proteins through charge complementarities, $\pi-\pi$ stacking, and other nonspecific interactions.[11−13] Carboxylated SWCNTs might interact with proteins located on the cell membrane or in the cytoplasm of multipotent mesenchymal stem cells, which have a further impact on subsequent cellular signaling pathways.[14] Recent studies have

* Address correspondence to jhsun@bjut.edu.cn or liangxj@nanoctr.cn.

Received for review March 31, 2012 and accepted November 21, 2012.

Published online November 21, 2012
10.1021/nn302457v

shown that bacterial membrane rhodopsin proteins (bR) can be adsorbed onto SWCNTs through hydrophobic interactions between the bR α-helices and the sidewall of the nanotube. This noncovalent functionalization caused bR proteins to undergo significant secondary structural changes.[15] These results suggest that an understanding of the effects of SWCNTs on protein conformation and function may be essential for developing novel biological and medical applications for SWCNTs.

Cytochrome *c* (Cyt *c*) is a key component of the mitochondrial respiratory chain that exists in the cytosol between the inner and outer membranes of mitochondria. The heme group of Cyt *c* allows it to undergo redox reactions. Cyt *c* plays an important role in the biological respiratory chain, whose function is to receive electrons from cytochrome *c* reductase and deliver them to cytochrome *c* oxidase. The activity of Cyt *c* is essential for mitochondrial function and is further associated with a variety of processes including cellular differentiation, apoptosis, control of the cell cycle, and cell growth.[16] Mitochondrial dysfunction leads to cell apoptosis and is closely linked with several diseases.[17,18] Cyt *c* is also involved in initiation of apoptosis by abnormal accumulation in cytoplasm, which initiates signal pathways leading to cell dysfunction.[19,20] The release of Cyt *c* from mitochondria into the cytoplasm has been shown to induce or activate apoptosis through interactions with cytoplasmic proteins such as apaf-1, Bcl-2, TIB, and caspase.[21] In addition, dysfunction of Cyt *c* can modulate the mitochondrial membrane potential (MMP) and cause mitochondrial respiratory chain malfunction.[22] SWCNTs have been demonstrated to promote the reduction/oxidation of cytochrome *c*.[23] In another study, SWCNTs were used as transporters to shuttle Cyt *c* through the plasma membrane and into the cytoplasm to regulate the activities of cells.[24]

SWCNTs were found to localize exclusively in the mitochondria of both tumor and normal cells.[25] To date, reports on whether SWCNTs themselves could affect the function and activity of Cyt *c* and the resulting effects on cellular functions are limited. Technically, it is very difficult to avoid aggregation of pristine SWCNTs when they are suspended in physiologically relevant solvents. This problem has hindered the progress of our understanding of the interactions between Cyt *c* and SWCNTs. In this study, we modified SWCNTs with carboxy groups to avoid their aggregation. The redox properties of Cyt *c* were examined following incubation with suspensions of SWCNTs in physiological buffer. For the first time, we demonstrate that the redox potential of Cyt *c* is altered by interacting with SWCNTs. In addition, the SWCNT treatment caused MMP change, and mitochondrial respiration inhibition in KB cells was measured. The results provide evidence that SWCNTs can cause MMP change and decrease the level of mitochondrial oxygen uptake in cells, which are the results of the redox activity change and impaired electron transfer of Cyt *c*. While the exact mechanism needs to be further explored, our studies of the interactions between SWCNTs and Cyt *c* provide some clues about how SWCNTs may interact with Cyt *c* and affect cellular functions.

RESULTS AND DISCUSSION

SWCNTs have been widely used to shuttle biomolecules including proteins, DNA, and siRNA into cells.[26−28] Whether the structure and function of these "passenger" molecules as well as cellular components can be affected by SWCNTs and how SWCNTs affect cellular activities need to be addressed. Because pristine SWCNTs have low solubility in water, we modified SWCNTs with carboxy groups and dispersed them in PB containing 0.5 wt % sodium cholate. The derived suspensions of individual SWCNTs have enhanced stability (Figure 1a, b). While pristine SWCNTs rapidly aggregated and precipitated out, carboxy-SWCNTs exhibited high suspension stability. We also tested the stability of carboxy-SWCNTs in complete DMEM media. As is shown in Figure S1, carboxy-SWCNTs exhibited high suspension stability in complete DMEM media. These stable suspensions of SWCNTs were used in studies on Cyt *c* to clarify how SWCNTs affect cellular activities and interact with Cyt *c*.

Cellular Uptake of SWCNTs and Mitochondrial Morphology Change. In order to monitor the entry of SWCNTs into cells under selected conditions, we employed the micro-Raman technique of the G-band of SWCNTs in KB cells with an approximately 2 mm spatial resolution. In Raman mapping images, the color change represents the content of carbon nanotubes in the cells. With the increase of SWCNTs content, the color of the Raman mapping images changes from black to orange. Figure 1c and d show the Raman mapping images of KB cells incubated with or without 60 μg/mL SWCNTs for 24 h. As expected, a strong Raman signal was observed at about 1580 cm^{-1} in KB cells after incubation with SWCNTs. In contrast, almost no obvious Raman signals were observed for control cells. The presence of SWCNTs is seen as an orange area in the cells by a Raman intensity ratio map. Raman mapping clearly indicates that SWCNTs entered and accumulated in KB cells with intensive near-infrared excited Raman signals.

It is known that SWCNTs exhibit a strong resonance Raman shift at about 1580 cm^{-1}, a specific characteristic graphitic stretching mode, which can be used to measure the quantity of SWCNTs. Therefore, we further examined the G band intensity of 1580 cm^{-1} in the isolated mitochondria of KB cells treated with SWCNTs from 0 to 60 μg/mL for 24 h. It was found that the mitochondrial targeting of SWCNTs is dose-dependent, with higher Raman intensities observed for SWCNT signals in the mitochondria isolated from cells treated with a higher SWCNT concentration (Figure 2A).

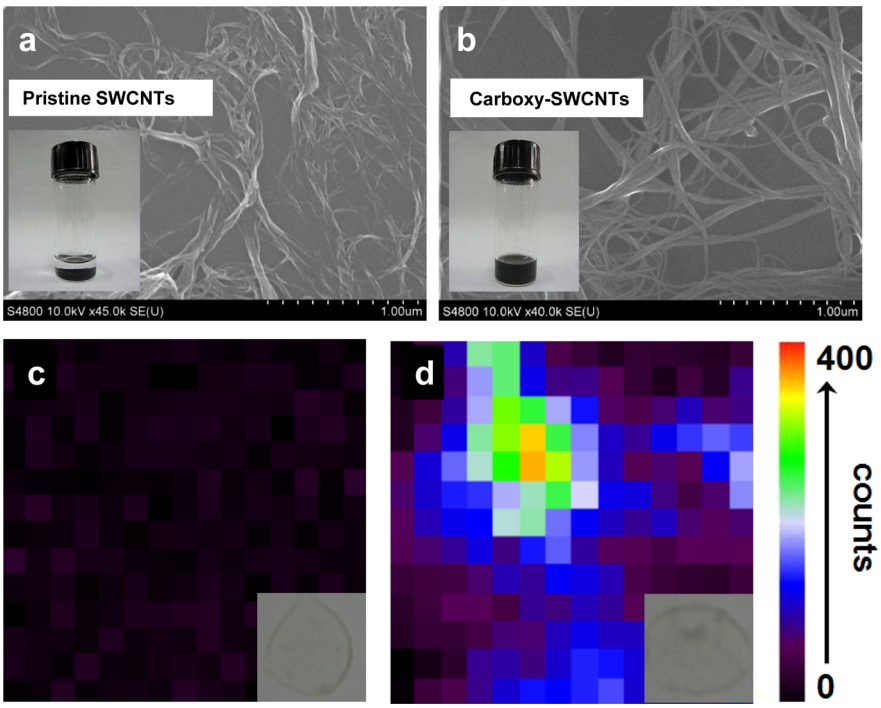

Figure 1. Characterization and cellular penetration of SWCNTs. TEM images and dispersion images of (a) pristine SWCNTs and (b) carboxy-SWCNTs. Raman mapping images of carboxy-SWCNT penetration into KB cells. G-mode (1580 cm^{-1}) Raman intensity images of SWCNTs in single KB cell (c) incubated in PB buffer as control for 24 h and (d) incubated with 60 μg/mL carboxyl-SWCNTs for 24 h. Inset: Regular optical microscope images of a KB cell. Scale is 10 $\times$ 10 μm.

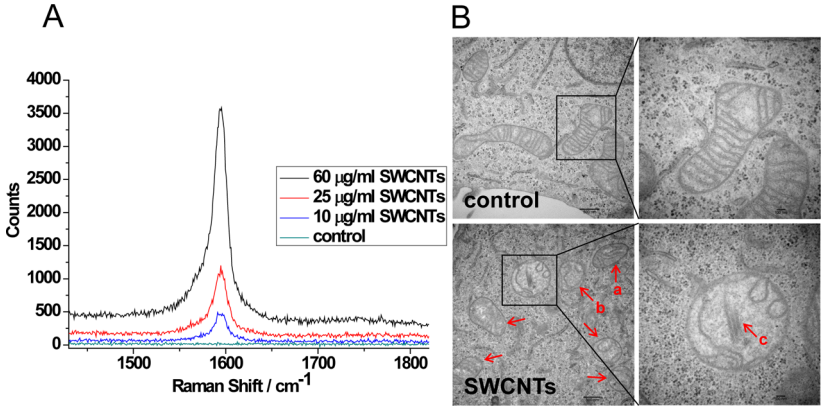

Figure 2. Entering of SWCNTs to the mitochondria and mitochondria structure change. (A) Raman spectra of isolated mitochondria of cells treated with different concentrations of SWCNTs from 0 to 60 μg/mL for 24 h. Curves represent G band (1580 cm^{-1}) Raman spectra of SWCNTs in mitochondria, extracted with a mitochondria isolation kit, measured with equal quantities. (B) Morphology of mitochondria of SWCNT-treated cells examined by transmission electron microscopy. Swelling of mitochondria is indicated by arrows. Arrow a: Mild mitochondrial damage; the cristae are smaller. Arrow b: Severe mitochondrial damage; the cristae are nearly completely destroyed or disappeared. Arrow c: SWCNTs located in a mitochondrion. Scale bar: 500 and 100 nm.

To verify the entering of SWCNTs to the mitochondria, we carried out transmission electron microscopy to observe the mitochondria in KB cells treated with 60 μg/mL of SWCNTs for 24 h. TEM images show that SWCNTs appeared in mitochondria (Figure 2B, arrow c), and the mitochondrial structure was greatly affected. The mitochondria became swollen and round, with the cristae appearing irregular and disordered. Some mitochondria became vacuolus, and the cristae were nearly completely destroyed or disappeared (Figure 2B). The morphology of mitochondria of KB cells treated with 20, 40, and 80 μg/mL of SWCNTs for 24 h is shown in Figure S2.

SWCNT Treatment Decreases the Level of Mitochondrial Oxygen Uptake. To measure whether SWCNTs can affect mitochondrial respiration, oxygen uptake was measured in KB cells in culture using a sensitive self-referencing oxygen electrode.[29] The oxygen consumption measurement is based on the translational movement of an oxygen-selective microelectrode at a known frequency through the gradient of the oxygen concentration

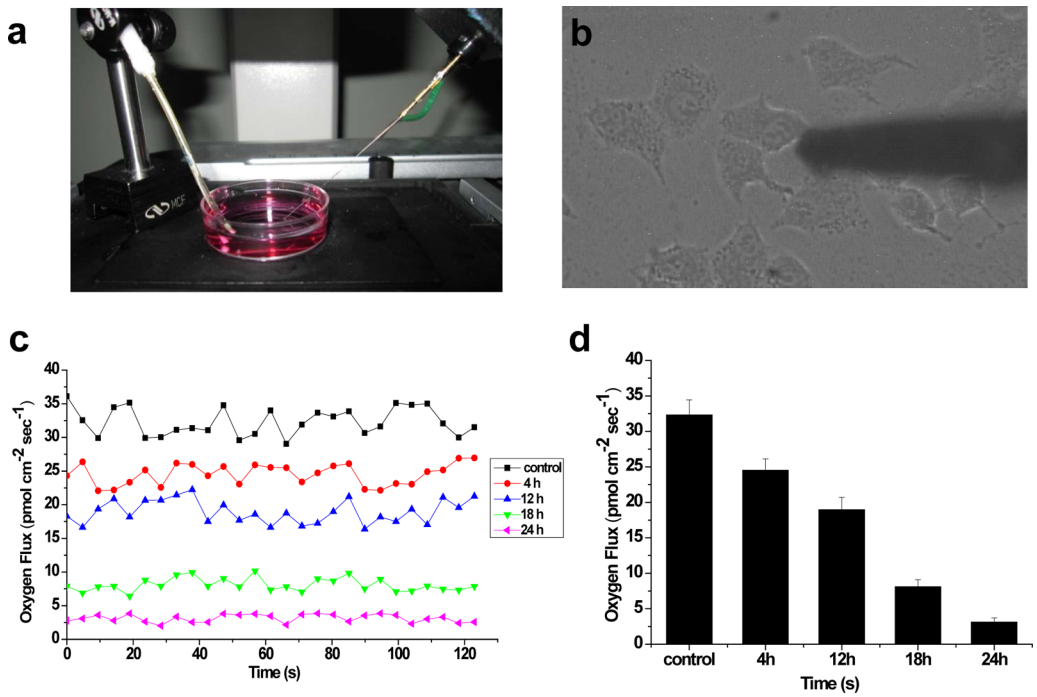

Figure 3. SWCNTs alter O_2 consumption by KB cells. (a) The self-reference electrode. The system is set up on top of a spinning disk confocal microscope. (b) Self-referencing electrode positioned next to a single KB cell. (c) Representative traces of oxygen flux levels of single KB cells. (d) Group data for basal respiration levels of single KB cells (control) or KB cells treated with 60 μg/mL SWCNTs from 4 to 24 h. At least three independent cultures were used for each study.

around the cell. The differential current of the electrode was converted into a directional measurement of oxygen flux using the Fick equation. Mitochondria require oxygen to produce ATP in sufficient quantities to drive energy-requiring reactions in eukaryotic organisms. The oxygen flux detected reliably correlates with the metabolic state of the cell. Normal mitochondria have high oxygen flux, and a lower level of oxygen flux is a result of malfunctioning mitochondria. As is shown in Figure 3c and d, oxygen consumption in KB cells declined after SWCNT treatment in a time-dependent manner. After 24 h of SWCNT treatment, the oxygen flux of cells is only about 9.7% of that in the control group. The result clearly shows that mitochondrial oxygen consumption of cells is significantly decreased by SWCNT treatment.

Effects of SWCNTs on Mitochondrial Membrane Potential. Mitochondria, one of the most important organelles in eukaryotic cells, furnish cellular energy through respiration and regulate cellular metabolism as a cellular power plant to maintain the growth, differentiation, and proliferation of cells. The effect of SWCNTs on mitochondrial function was investigated by examining their effects on the MMP, an indicator of mitochondrial activity. We used the MTT assay to evaluate the effect of different concentrations of SWCNTs on cell viability. Our results show that the viability of KB cells decreased after exposure to SWCNTs dispersion for 24 h at high concentrations, while the viability was not significantly affected by PB buffer containing sodium cholate with the same concentration (Figure S3). Sodium cholate is a surfactant of low biological toxicity broadly used to disperse SWCNTs.[30] Cells treated with 60 μg/mL SWCNTs, which would result in 70% cell viability after 24 h of exposure, were used to investigate the effects of SWCNTs to mitochondria.

The effect of SWCNTs on the MMP of KB cells was first measured by flow cytometry with JC-1 staining. JC-1 existed either as a green fluorescent monomer at depolarized membrane potentials or as a red fluorescent J-aggregate at hyperpolarized membrane potentials. Changed MMPs were indicated by a fluorescence emission shift from J-aggregates with red fluorescence (~590 nm) to J-monomers with green fluorescence (~529 nm). The higher mitochondrial membrane potentials were defined by the higher ratio of red fluorescent intensity and green fluorescent intensity.[31] Flow cytometry results are expressed as a decrease or increase of fluorescence intensity, indicating a change of MMP among cell populations (Figure 4). Cells incubated with 60 μg/mL SWCNTs showed a decrease of the red fluorescence intensity in a time-dependent manner. Carbonyl cyanide 3-chlorophenyl hydrazone (CCCP), an uncoupled agent that depolarizes mitochondrial membranes, was used as a positive control. The CCCP-treated group showed a dramatic decrease of red fluorescence intensity (Figure 4b). Cells in the R_2 region have normal MMP, while those in the R_3 region have reduced MMP. The percentages appearing in each panel of Figure 4 are the percentages of cells in

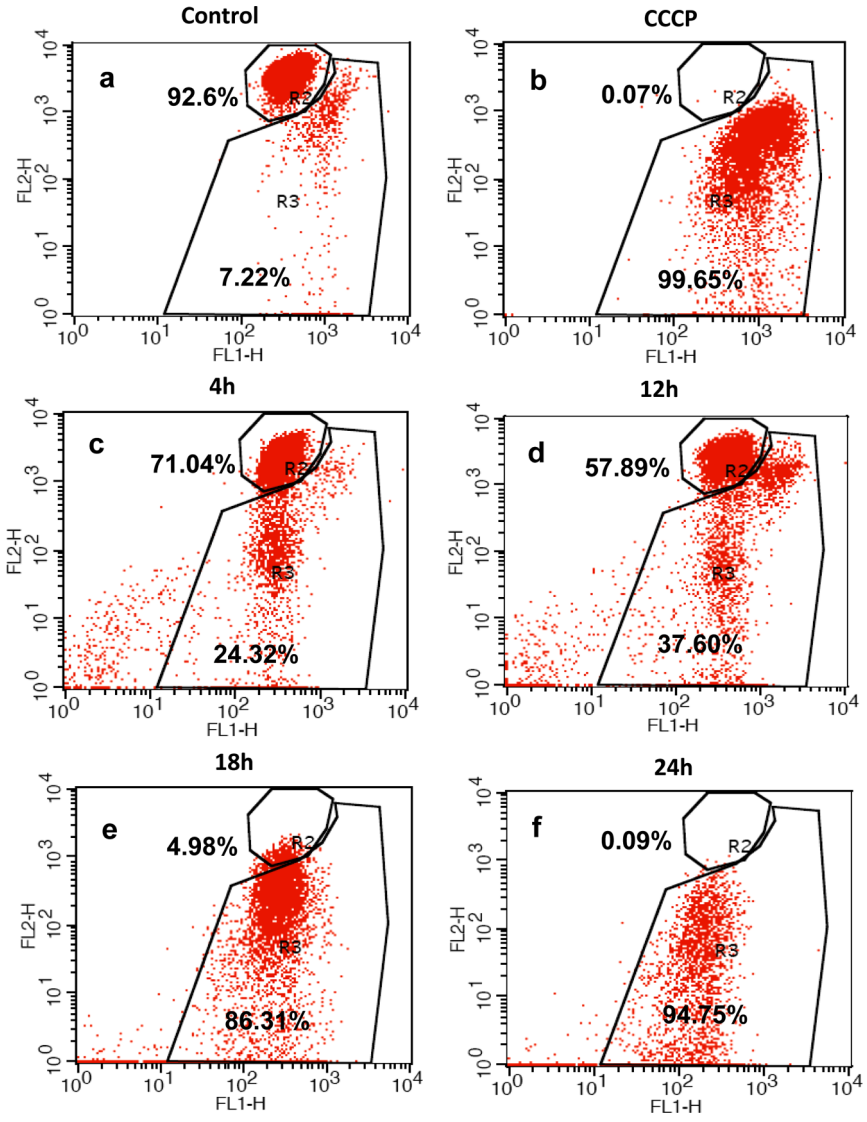

Figure 4. SWCNT treatment significantly triggered MMP decrease. Changes of MMP in KB cells were examined by flow cytometry. (a) KB cells were cultured in DMEM media as control. (b) KB cells treated with CCCP were used as a positive control. (c–f) Cells were treated with 60 μg/mL of SWCNTs for 4, 12, 18, and 24 h. The numbers indicate the percentage of KB cells with undepolarized (R_2) or depolarized (R_3) membrane potential.

the R_2 and R_3 regions. The results show that the longer KB cells are incubated with SWCNTs, the more cells exhibit a depolarized MMP. When cells were incubated with SWCNTs for 24 h, the MMP of 94.75% of cells was depolarized (Figure 4f).

To confirm the results obtained from flow cytometry, we examined the change of fluorescence in mitochondria by confocal microscopy. The MMP of KB cells in the presence or absence of SWCNTs was measured by confocal microscopy after staining with JC-1 (Figure 5). Control cells had both red and green fluorescence, coexisting in the same cell (Figure 5, top panels). Superimposition of the green and red fluorescent images revealed a large degree of overlap and displayed an orange color. Treatment with the positive control, CCCP, dramatically decreased the red fluorescence (Figure 5, middle panels) and caused a visible increase of the green fluorescence intensity. The shift in membrane potential was observed by disappearance of fluorescent red-stained mitochondria and an increase in fluorescent green-stained mitochondria. Following treatment with SWCNTs, formation of red fluorescent J-aggregates decreased, and the ratio of red fluorescence intensity to green fluorescence intensity decreased gradually (Figure 5, bottom panels), indicating increased depolarization of mitochondria with prolonged exposure to SWCNTs. These results are consistent with the results obtained using flow cytometry.

SWCNT Treatment Increases the ROS Level in Cells. It has been reported that Cyt *c* plays an important role in ROS clearance.[32,33] The intracellular ROS level of cells treated with SWCNTs was measured after treating the KB cells with 60 μg/mL SWCNTs for 24 h. As shown in Figure S4, compared with the control group, an enhanced ROS level

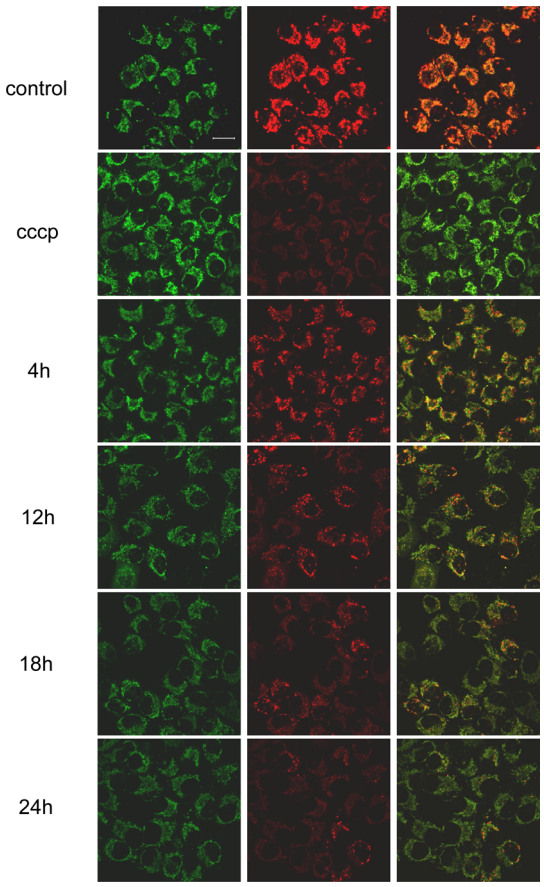

Figure 5. Mitochondrial depolarization imaged by confocal microscopy. MMP of cells stained with JC-1 dye was measured with confocal microscopy. Left and middle images showed the fluorescence of green fluorescent J-monomer and red fluorescent J-aggregate, respectively. The right images showed the overlay of two images. The results were consistent with FACS quantitative measurements. Scale bar: 20 μm.

was detected in SWCNTs-treated cells, which is direct evidence of mitochondrial electron transport disruption and blocked respiratory chain activity.

Interaction of SWCNTs with Cyt *c*. Normal mitochondrial function requires the balanced interaction between many critical mitochondrial proteins. Minor changes of these proteins could result in dramatic effects on cellular metabolism. Cyt *c* plays an important role in mitochondrial electron transport and cell metabolism. Its role in maintaining a normal MMP is well established.[34] Cyt *c* is a well-characterized, small, heme-containing redox protein with a molecular weight of 12.384 g/mol. The heme edge of Cyt *c* is surrounded by an array of lysine and arginine residues. Cyt *c* transfers electrons by undergoing oxidation and reduction of the iron cation (which can be alternately 2+ or 3+) in Cyt *c*'s heme moiety. Oxidized Cyt *c* has absorption peaks at 408 and 530 nm, while reduced Cyt *c* has three peaks, at 415, 520, and 550 nm.[35] The additional peak at 550 nm can, therefore, be monitored spectroscopically to quantitate the amount of reduced Cyt *c*. We determined that Cyt *c* could bind onto SWCNTs (Figure S5). The extent of binding depended on the concentrations of both Cyt *c* and SWCNTs. The amount of Cyt *c* binding with SWCNTs was quantified with UV−visible spectra at 408 nm. When the concentration of Cyt *c* was changed, the amount of Cyt *c* bound to 100 μg/mL SWCNTs showed a linear increase and reached a maximum at 150 μg/mL (Figure S5). The adsorption of Cyt *c* onto SWCNTs is shown in Figure S6.

Systematic spectroscopic studies were conducted to explore the interaction between Cyt *c* and SWCNTs. First, it was found that a new absorption peak at 550 nm, the characteristic peak of reduced Cyt *c*, appeared in the presence of SWCNTs (Figure 6a), similar to the positive control of ascorbic acid, which reduces Cyt *c* rapidly and thoroughly (Figure S7). This result clearly demonstrates that Cyt *c* undergoes reduction in the presence of SWCNTs. Next, the effect of pH on the interaction between SWCNTs and Cyt *c* was investigated. A solution with Cyt *c* was used as a control. Reduction of Cyt *c* was facilitated when the pH increased from 7.0 to 9.0, consistent with an increase in the absorbance at 550 nm (Figure 6b). In order to prove this phenomenon was caused only by SWCNTs, the effects of sodium cholate and ionic strength, the other two components in this system, on Cyt *c* reduction were evaluated at pH 7.0. There was no peak at 550 nm when the concentration of sodium cholate increased from 0.25 wt % to 2.0 wt %, indicating that sodium cholate had little effect on the reduction (Figure S8a). The effect of PB on the interaction between SWCNTs and Cyt *c* was also investigated. The change of PB concentration from 10 mM to 50 mM had no significant effect on the interaction of SWCNTs with Cyt *c* (Figure S8b). Taken together, these results demonstrate that the reduction of Cyt *c* is caused only by SWCNTs and that this reduction is enhanced by an increase of pH.

To find out whether the nonspecific adsorption of serum proteins onto the SWCNT surface will affect their interaction with Cyt *c*, we also carried out the experiment in complete DMEM media. It was found that Cyt *c* can still be reduced by SWCNTs in complete DMEM media (Figure S9).

Mechanism of the Interaction of SWCNTs with Cyt *c*. To analyze the underlying mechanism of the interaction between Cyt *c* and SWCNTs, we further examined the structural change of Cyt *c* at different pH's. It has been reported that the structure of Cyt *c* changes in alkaline solutions. This conformational change is thought to increase the exposure of Cyt *c*'s heme group to the solvent.[36,37] In this study, the reduction of Cyt *c* by SWCNTs was enhanced under alkaline conditions. This observation raises the possibility that, at alkaline pH, SWCNTs can more easily access the heme group of Cyt *c*, resulting in facilitated reduction of Cyt *c*.

To test this hypothesis, the effect of pH on the conformation change of Cyt *c* was measured using circular dichroism.[38] We found that the α-helical content of Cyt *c* decreased from 29.9% to 25.8% (pH 7.0

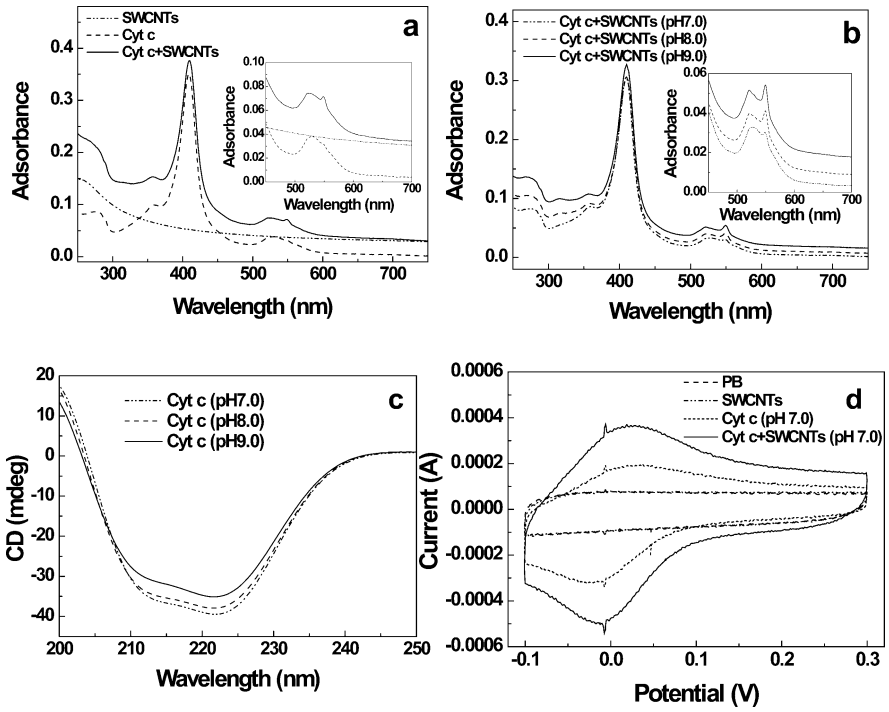

Figure 6. Interaction of SWCNTs with Cyt *c* was indicated with different measurements. (a) UV−vis spectra of Cyt *c*, SWCNTs, and SWCNT + Cyt *c*. The absorption spectrum was magnified in the inset graph as a characteristic peak of Cyt *c* at 550 nm. (b) UV−vis spectra of Cyt *c* under interaction with SWCNTs at different pH's from 7.0 to 9.0. The adsorption spectrum was magnified in the inset graph as a characteristic peak of Cyt *c* at 550 nm. (c) CD spectra of Cyt *c* at different pH's from 7.0 to 9.0. (d) Cyclic voltammograms of Cyt *c* (150 μg/mL) measured with or without SWCNTs (100 μg/mL) and 10 mM PB at pH 7.0. Scan rate = 50 mV s^{-1}.

and pH 8.0, respectively) and to 23.1% (pH 9.0) when the pH was raised (Figure 6c). The distal loop region moved away from the heme moiety at alkaline pH to form a channel with a heme group.[36] As the pH increases, the heme group of Cyt *c* was exposed to the solvent to a greater extent, which makes SWCNTs more accessible to the heme group and thereby increases the percentage of Cyt *c* being reduced. The structure change of Cyt *c* opened a channel to the heme pocket through the α-helix and allowed SWCNTs an easier access to the heme group through this channel at higher pH. In addition to the CD measurement, the redox potential of Cyt *c* was determined using cyclic voltammetry (CV). The results of the CV measurements indicated that Cyt *c* had a pair of redox peaks and its redox potential was significantly enhanced in the presence of SWCNTs (Figure 6d). On the basis of CD results and CV results, the structure of Cyt *c* was changed, which increased the exposure of the heme moiety to the solvent, and then the reduction activity became more obvious in the presence of SWCNTs.

To better understand the effects of SWCNTs on the electron transfer of Cyt *c*, the ability of Cyt *c* to catalyze the oxidation of 5,5-dimethyl *N*-oxide pyrroline (DMPO) to 5,5-dimethyl-1-pyrrolidone-*N*-oxyl (DMPOX) was studied using the electron spin resonance (ESR) technique. In the presence of Cyt *c*, H_2O_2 caused the oxidation of DMPO to DMPOX, which gave the typical seven-line ESR spectrum shown as an inset in Figure 7, and the intensity of the second line in the ESR spectrum of DMPOX was used to monitor the time dependence. Ascorbic acid, as a positive control, inhibited this oxidation in a concentration-dependent manner (Figure 7a). This inhibition was observed as a delay in the appearance of the ESR signal for DMPOX. Similarly, addition of SWCNTs also resulted in a similar concentration-dependent inhibition of oxidation (Figure 7b). As the SWCNT concentration increased, the phenomenon of the ESR signal delay for DMPOX became more obvious with the appearance time from about 150 to 350 s and lowered the intensity from 10.5 to 4.5 au, indicating the slower and smaller amount of electron being transferred. These results indicated that SWCNTs can affect the electron transfer and catalytic ability of Cyt *c* required for the oxidation of DMPO to DMPOX.

Mitochondria are the powerhouses of the living cell, generating energy for various cellular activities. The function and integrity of mitochondria may impact the viability, proliferation/division, and hypoxic tolerance of the cell, and mitochondrial dysfunction is implicated in the pathogenesis of many diseases. For this reason, the study of mitochondrial function has become central to a wide variety of clinical and basic science research. The majority of ATP generation is dependent on mitochondrial electron transport. Cyt *c*, as an integral mitochondrial protein, plays an important role in electron transport and cell respiration.[34] Cytochrome *c*

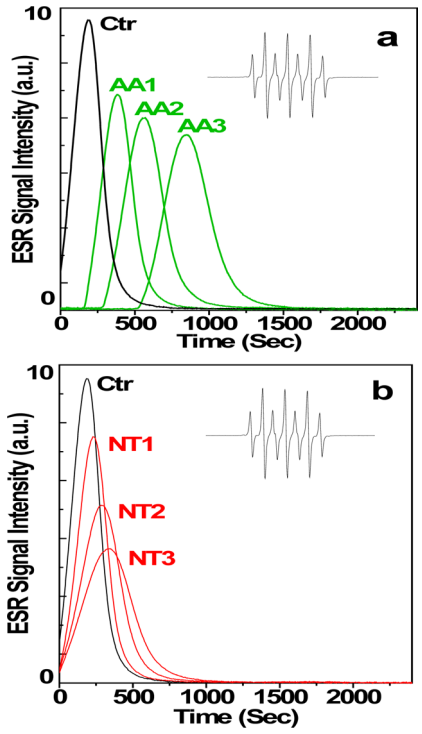

Figure 7. Time-dependent ESR signal of DMPOX measured during oxidation of the spin trap DMPO by Cyt *c*/H_2O_2 at ambient temperature. The intensity of the second line in the ESR spectrum of DMPOX was used to monitor the time dependence. (a) Time dependence of the ESR signal for solutions containing 50 mM DMPO, 0.1 mM Cyt *c*, and 0.5 mM H_2O_2 without (Ctr: control) or with ascorbic acid (AA1: 0.01 mM ascorbic acid; AA2: 0.05 mM ascorbic acid; AA3: 0.1 mM ascorbic acid) measured at pH 7.0. (b) Time dependence of the ESR signal with 10 μg/mL SWCNTs (NT1: 2.5 μL; NT2: 5 μL; NT3: 7.5 μL), substituted for ascorbic acid, measured at pH 7.0. The typical seven-line ESR spectrum of DMPOX is given as the inset after oxidation of DMPO in the presence of Cyt *c* and H_2O_2.

oxidase is the terminal enzyme of the mitochondrial respiratory chain and is responsible for 90% of cellular oxygen consumption in mammals. In mitochondria, cytochrome *c* plays an essential role in the generation of MMP. This potential is essential for various functions including the production of ATP *via* oxidative phosphorylation.

To successfully apply the new generation of nanomaterials as drug carriers in the treatment of diseases, it is essential to determine their pharmacological and toxicological profiles. SWCNTs are commonly used as carriers to forward different payloads into cells. However, as the basis of biomedical applications of SWCNTs, their interactions with intracellular molecules in cells have not been fully understood. The potential biomedical applications of nanotubes require a better understanding of their cellular dynamics for their better usage in the clinic. The toxicity of carbon nanotubes has been an important issue in carbon nanomaterial research. The potential cytotoxicity includes metabolic pathway disruption, redox regulation, cytoskeleton formation alteration, cell growth inhibiton, *etc*. Yuan *et al*. found that two cytoskeleton -related proteins, profilin and filamin, were upregulated by approximately 35% in oxidized SWCNT-treated cells. The upregulation of these cytoskeleton proteins suggested that the exposure of SWCNTs might alter the intracellular microfilament network.[39] Kagan *et al*. demonstrated that iron-rich SWCNTs caused a significant loss of intracellular low molecular weight thiols and accumulation of lipid hydroperoxides in murine macrophages.[40] It has been reported that mitochondria are the target organelles for the cytotoxicity of SWCNTs.[41] Consistent with the reports of other investigators, we have found that treatment of cells with SWCNTs resulted in accumulation of the SWCNTs in the cells. At low concentrations, for short periods, SWCNTs inhibit cytochrome *c* oxidase to a lower extent, but a higher period of SWCNT exposure results in inhibition of respiration, leading to the development of "metabolic hypoxia", a situation in which, although oxygen is available, the cell is unable to utilize it. We have further determined that this accumulation of SWCNTs was accompanied by a reduction in the MMP. Cytochrome *c* molecules can be successfully absorbed noncovalently on carbon nanotubes.[42] The interaction most likely occurs *via* the protein side that is rich in Lys residues, since the primary amines strongly bind to carboxylate functionalities, and amines are also known to strongly interact with the carbon-nanotube sidewall.[43] The effect of SWCNTs on the electron-transfer reaction of cytochrome *c* has been previously studied in biosensor research. Wang *et al*. has found the activated SWCNT-modified electrode promotes the reduction/oxidation of cytochrome *c*.[23] Our results suggest that SWCNTs may directly interact with Cyt *c* to alter its oxidation state and redox potential, resulting in an alteration in Cyt *c*'s ability to facilitate electron transport. Disruption in electron transfer has many unfavorable conquences. It has been reported that disrupting electron transfer at cytochrome *c* oxidase may result in ionic readjustment and modulation of the Ca^{2+} flux between the mitochondria and the endoplasmic reticulum.[44]

CONCLUSIONS

In this study, we investigated the effect of SWCNTs on mitochondria function and the interactions of SWCNTs with Cyt *c*, an important component of the electron transport chain in mitochondria. On the basis of the extracellular interactions of cytochrome *c* with carbon nanotubes, and the intracellular mitochondrial dysfunction induced by SWCNT treatment, we primarily conclude that the effects of SWCNTs on mitochondria should be a stepwise process: (1) SWCNTs enter the cells and localize in the mitochondria; (2) Cyt *c* is partially reduced when interacting with SWCNTs and the redox activity of Cyt *c* is affected; (3) the electron transfer of Cyt *c* is decreased and attenuated; (4) MMP is decreased; (5) the mitochondrial respiratory chain is disrupted and mitochondrial oxygen uptake is greatly reduced; (6) metabolic hypoxia is caused by SWCNTs

and the mitochondrial electron transport-dependent ATP generation is affected. Identification of pharmacological and toxicological profiles is of critical importance for the use of nanoparticles as drug carriers in nanomedicine and for the biosafety evaluation of environmental nanoparticles in nanotoxicology. The findings of this study will broaden and deepen our understanding of the interaction of SWCNTs with Cyt *c* and the mechanism of mitochondria dysfunction caused by SWCNTs. When using SWCNTs to fulfill different applications such as live imaging, photothermal therapy, and pharmaceutical carriers in the future, their disruption of mitochondria function and cellular respiration should be considered.

METHODS

Materials. Pristine SWCNTs were purchased from Chengdu Organic Chemicals Company Ltd. of Chinese Academy of Sciences. Carbonyl cyanide 3-chlorophenyl hydrazone (CCCP) and sodium cholate were obtained from Alfa Aesar (Ward Hill, MA, USA). Oxidized Cyt *c* from horse heart, the spin trap, 5,5-dimethyl *N*-oxide pyrroline (DMPO), and L-ascorbic acid were purchased from Sigma (St. Louis, MO, USA). Mitochondria were isolated by a Mitochondria Isolation Kit (Pierce, Rockford, IL, USA) for cultured cells. All chemicals were of analytical grade and were used without further purification.

Preparation of Carboxyl-SWCNTs. In order to improve their dispersity and stability in solutions, pristine SWCNTs were treated by acid oxidation. Briefly, 0.1 g of pristine SWCNTs and 100 mL of a 3:1 (v/v) mixture of 98% H_2SO_4 and 68% HNO_3 were mixed and sonicated for 2 h. The resulting dark suspension was cooled to room temperature and diluted with distilled water. The diluted suspension was filtered through a 0.22 μm polycarbonate membrane (Millipore, USA) and rinsed with distilled water until the pH was greater than 5. Finally, the purified carboxy-SWCNTs were dried at room temperature. Carboxyl-SWCNTs were suspended in phosphate buffer (30 mM, pH 7.0) with 0.5 wt % sodium cholate surfactant and sonicated for 2 h. The suspension was then centrifuged at 1500 rpm for 10 min to remove large bundles. The concentration of carboxyl-SWCNTs was determined by UV−visible spectroscopy.

MTT Assay. The cell viability of human epithelial carcinoma cells (KB cells, kindly provided by Dr. Michael M. Gottesman, CCR, NCI) treated with SWCNTs was determined using the MTT assay. Cells were stained with 100 μL of sterilized MTT dye ((3-(4,5-dimethylthiazol-2-yl)-2,5-diphenyltetrazolium bromide, 0.5 mg/mL, Sigma-Aldrich) for 4 h at 37 °C, and 100 μL of DMSO was added. The spectrometric absorbance at 570 nm was measured on a microplate reader (M200, Tecan, Männedorf, Switzerland).

Micro-Raman Mapping. After 24 h of treatment with SWCNTs, KB cells were washed twice to remove free SWCNTs, and the media was replaced with PBS. The scanning area was selected by focusing on the cells using the microscope, and the micro-Raman laser was then focused on the dish (λ excitation = 785 nm) using the Renishaw micro-Raman spectroscopy system (Renishaw plc, Wotton-under-Edge, UK). A line scanning mode was applied to get a Raman spectrum at every point in the selected area (1 μm × 1 μm for each point). The image was obtained by plotting the integrated area in the range 1580−1610 cm^{-1} of the Raman spectra obtained in the cell-containing area.

Oxygen Flux Measurements. Oxygen consumption was recorded according to the self-referencing method.[29,45] Briefly, a platinum electrode was placed 5 μm from the cell and then moved rapidly back and forth over a 10 μm distance between two points located 5 and 15 μm away from the cell soma in the X−Y axes, so that the oxygen-sensing electrode was positioned repeatedly closer to and farther from the cell. This amperometric probe was polarized with −0.6 V, at which voltage the reduction of oxygen at the probe tip was diffusion-limiting, and therefore $[O_2]$ in the solution could be assessed. As the O_2 concentration near the cell is smaller than in the far position, the difference in current between the near and the far position of the platinum electrode represents the gradient of the oxygen concentration around the cell, a reflection of O_2 consumption. We then converted the difference in current into oxygen flux . The oxygen flux level was measured every 4.73 s. Figure 3c is the representative trace of the oxygen flux level of one single cell under each treatment. Figure 3d is the average oxygen flux value of all the measured values of all the cells under each treatment.

Flow Cytometry Measurements. The MMP was measured with 1.5 μM JC-1 (5,5′,6,6′-tetrachloro-1,1′,3,3′-tetraethylbenzimidazolylcarbocyanine iodide) (Invitrogen, Rockville, MD, USA) by flow cytometry. KB cells were seeded in six-well plates and incubated for 24 h. Then cells were incubated in fresh DMEM media or in media containing SWCNTs for 4, 12, 18, and 24 h. As a known MMP disrupter, 100 μM carbonyl cyanide 3-chlorophenyl hydrazone (CCCP, Alfa Aesar, Haverhill, MA, USA) was used as a positive control. After incubation, cells were trypsinized, collected by centrifugation, and then incubated with medium containing JC-1 dye for 20 min at 37 °C. Finally, the cells were washed and resuspended in 1 mL of PBS for fluorescent analysis using a FACScan flow cytometer. J-aggregate fluorescence was recorded by flow cytometry in fluorescence channel 2 (FL2) and monomer fluorescence in fluorescence channel 1 (FL1).

Confocal Microscopy Imaging. KB cells were seeded in polylysine-coated glass bottom dishes. After 24 h, the cells were treated with SWCNTs for 4, 12, 18, and 24 h. The cells were then stained with JC-1 dye as previously described for flow cytometry and examined by confocal microscopy (Ultraview VOX, Perkin-Elmer, Waltham, MA, USA).

Measurement of Interactions between Cyt *c* and Carboxyl-SWCNTs. Cyt *c* was incubated with selected concentrations of carboxyl-SWCNTs for 1 h at room temperature. After incubation, the suspension was centrifuged at 13 000 rpm for 30 min, and the supernatant was removed. The amount of Cyt *c* in the supernatant was measured using UV−visible spectroscopy (Lambda 950, Perkin-Elmer, USA). The UV absorption peak at 408 nm, attributable to the heme group in the Soret region of the Cyt *c* spectrum, was used to quantitate Cyt *c*.

UV−Visible Spectroscopy Assay. The reduction of oxidized Cyt *c* in the presence of SWCNTs was measured using the absorption of Cyt *c* at 550 nm characteristic for reduced Cyt *c*. Ascorbic acid, a known reducing agent, was used as a positive control. Briefly, oxidized Cyt *c* was dissolved in PB solution. The spectra were measured after SWCNTs (0.1 mg/mL) or ascorbic acid (5 mg/mL) was added. In addition, to measure the effect of the surfactant, sodium cholate, on the reduction of Cyt *c* by SWCNTs, UV−visible absorption spectra were obtained for solutions containing Cyt *c* (150 μg/mL), SWCNTs (100 μg/mL), and sodium cholate ranging from 0.25 to 2 wt %. To study the effect of pH on the interaction between SWCNTs and Cyt *c*, SWCNTs (100 μg/mL) were incubated with oxidized Cyt *c* (150 μg/mL) in PB with increasing pH from 7.0 to 9.0.

Circular Dichroism (CD) Measurement. CD spectra in the far-UV (200−250 nm), near-UV (250−350 nm), and the Soret (350−450 nm) spectral regions were recorded using a spectropolarimeter (J-720, Jasco). Spectra were obtained for samples containing 600 μg/mL oxidized Cyt *c* in the absence or presence of SWCNTs (400 μg/mL) at different pH. CD spectra were measured using quartz cells with a 1 mm path length. All spectra were corrected for background absorption. Each experiment was repeated three times with a bandwidth of 1.0 nm and scanning rate of 100 nm/min. All the measurements were performed at a constant temperature of 20 °C.

Cyclic Voltammetry Analysis. A three-electrode cell with indium tin oxides (ITO) as working electrode, Pt as counter electrode, and Hg/Hg_2Cl_2 as reference electrode was used for the

measurements by potentiostat with PHE200TM physical electrochemistry analysis (Gamry Instruments, Warminster, PA, USA). The working electrode area was identical among samples. The cyclic voltammograms were recorded immediately after inserting the reference electrode into the potentiostat analyte solution (Princeton Applied Research, Oak Ridge, TN, USA). The potential cycling was started at 0.3 V and allowed to proceed until −0.1 V, and the cycle was completed by stopping the scan at 0.3 V (scan rate 50 mV/s).

Electron Spin Resonance Measurements. Oxidation of the spin trap DMPO, to form DMPOX, was monitored by ESR to determine the effects of SWCNTs on Cyt *c*'s ability to catalyze oxidation of substrates by H_2O_2. Conventional ESR spectra were obtained using a Bruker EMX ESR spectrometer (Billerica, MA, USA). ESR spectral measurements were obtained using the following settings: 10 mW microwave power, 1 G field modulation, and 100 G scan range The time dependence of the ESR signal for solutions containing 50 mM DMPO, 0.1 mM Cyt *c*, and 0.5 mM H_2O_2 with or without ascorbic acid (from 0.01 to 0.1 mM) was measured. Similarly, the time dependence of the ESR signal with 10 μg/mL SWCNTs (from 2.5 to 7.5 μL), substituted for ascorbic acid, was measured. The time dependence of the ESR signal intensity was obtained at a fixed field position (the peak position of the center line of ESR spectrum). Data collection began 1 min after sample mixing. For measurement of the time dependence of the ESR signal, a scan time of 30 min at the described fixed field position was used. All measurements were performed in triplicates at ambient temperature.

ROS Levels Detection. The cells treated with or without SWCNTs for 24 h were stained for 30 min with a 10 μM ROS probe DCFH-DA (Molecular Probes, Eugene, Oregen, USA) in PBS solution with 0.4% glucose. After the free probes were washed, the cells were observed using fluorescence microscopy.

Conflict of Interest: The authors declare no competing financial interest.

Supporting Information Available: Stability of carboxy-SWCNTs in physiological buffer and media; effect of SWCNTs and sodium cholate on the viability of KB cells; fluorescence microscopy images of ROS generation in SWCNT-treated KB cells; quantification of Cyt *c* absorbed onto SWCNTs; UV−visible spectra of Cyt *c* in the absence and presence of ascorbic acid; UV−visible spectra of Cyt *c* interacting with SWCNTs in the presence of different concentrations of sodium cholate; UV−visible spectra of Cyt *c* interacting with SWCNTs at pH 7.0 with varied PB concentration; and UV−vis spectra of Cyt *c* interacting with SWCNTs in complete DMEM media. These materials are available free of charge *via* the Internet at http://pubs.acs.org.

Acknowledgment. This work was supported by grants from the Chinese Natural Science Foundation project (Nos. 30970784 and 81171455), National Key Basic Research Program of China (2009CB930200), Chinese Academy of Sciences (CAS) "Hundred Talents Program" (07165111ZX), and CAS Knowledge Innovation Program. This work was supported in part by NIH/NCRR 3 G12 RR003048, NIH/NIMHD 8 G12 MD007597, and USAMRMC W81XWH-10-1-0767 grants. This article is not an official U.S. Food and Drug Administration (FDA) guidance or policy statement. No official support or endorsement by the U.S. FDA is intended or should be inferred. This work was supported by a regulatory science grant under the FY11 FDA Nanotechnology CORES Program (J.J.Y. and W.G.W.).

REFERENCES AND NOTES

1. Liu, Z.; Tabakman, S.; Welsher, K.; Dai, H. J. Carbon Nanotubes in Biology and Medicine: *In Vitro* and *in Vivo* Detection, Imaging and Drug Delivery. *Nano Res.* **2009**, *2*, 85–120.
2. Prato, M.; Kostarelos, K.; Bianco, A. Functionalized Carbon Nanotubes in Drug Design and Discovery. *Acc. Chem. Res.* **2008**, *41*, 60–68.
3. Zhou, F.; Xing, D.; Wu, B.; Wu, S.; Ou, Z.; Chen, W. R. New Insights of Transmembranal Mechanism and Subcellular Localization of Noncovalently Modified Single-Walled Carbon Nanotubes. *Nano Lett.* **2010**, *10*, 1677–1681.
4. Bayraktar, H.; Ghosh, P. S.; Rotello, V. M.; Knapp, M. J. Disruption of Protein-Protein Interactions Using Nanoparticles: Inhibition of Cytochrome C Peroxidase. *Chem. Commun. (Cambridge, U.K.)* **2006**, 1390–1392.
5. Karajanagi, S. S.; Vertegel, A. A.; Kane, R. S.; Dordick, J. S. Structure and Function of Enzymes Adsorbed onto Single-Walled Carbon Nanotubes. *Langmuir* **2004**, *20*, 11594–11599.
6. Zhang, B.; Xing, Y.; Li, Z.; Zhou, H.; Mu, Q.; Yan, B. Functionalized Carbon Nanotubes Specifically Bind to Alpha-Chymotrypsin's Catalytic Site and Regulate Its Enzymatic Function. *Nano Lett.* **2009**, *9*, 2280–2284.
7. Wijaya, I.; Gandhi, S.; Nie, T.; Wangoo, N.; Rodriguez, I.; Shekhawat, G.; Suri, C.; Mhaisalkar, S. Protein/Carbon Nanotubes Interaction: The Effect of Carboxylic Groups on Conformational and Conductance Changes. *Appl. Phys. Lett.* **2009**, *95*, 073704.
8. Yi, C.; Fong, C.; Zhang, Q.; Lee, S.; Yang, M. The Structure and Function of Ribonuclease A upon Interacting with Carbon Nanotubes. *Nanotechnology* **2008**, *19*, 095102.
9. Bayraktar, H.; You, C. C.; Rotello, V. M.; Knapp, M. J. Facial Control of Nanoparticle Binding to Cytochrome *c*. *J. Am. Chem. Soc.* **2007**, *129*, 2732–2733.
10. Sandanaraj, B.; Bayraktar, H.; Krishnamoorthy, K.; Knapp, M.; Thayumanavan, S. Recognition and Modulation of Cytochrome *c*'s Redox Properties Using an Amphiphilic Homopolymer. *Langmuir* **2007**, *23*, 3891–3897.
11. Shang, W.; Nuffer, J. H.; Dordick, J. S.; Siegel, R. W. Unfolding of Ribonuclease A on Silica Nanoparticle Surfaces. *Nano Lett.* **2007**, *7*, 1991–1995.
12. Cedervall, T.; Lynch, I.; Lindman, S.; Berggard, T.; Thulin, E.; Nilsson, H.; Dawson, K. A.; Linse, S. Understanding the Nanoparticle-Protein Corona using Methods to Quantify Exchange Rates and Affinities of Proteins for Nanoparticles. *Proc. Natl. Acad. Sci. U. S. A.* **2007**, *104*, 2050–2055.
13. Yi, C.; Fong, C.; Chen, W.; Qi, S.; Tzang, C.; Lee, S.; Yang, M. Interactions between Carbon Nanotubes and DNA Polymerase and Restriction Endonucleases. *Nanotechnology* **2007**, *18*, 025102.
14. Liu, D.; Yi, C.; Zhang, D.; Zhang, J.; Yang, M. Inhibition of Proliferation and Differentiation of Mesenchymal Stem Cells by Carboxylated Carbon Nanotubes. *ACS Nano* **2010**, *4*, 2185–2195.
15. Bertoncini, P.; Chauvet, O. Conformational Structural Changes of Bacteriorhodopsin Adsorbed onto Single-Walled Carbon Nanotubes. *J. Phys. Chem. B* **2010**, *114*, 4345–4350.
16. Li, K.; Li, Y.; Shelton, J. M.; Richardson, J. A.; Spencer, E.; Chen, Z. J.; Wang, X.; Williams, R. S. Cytochrome c Deficiency Causes Embryonic Lethality and Attenuates Stress-Induced Apoptosis. *Cell* **2000**, *101*, 389–399.
17. Maloyan, A.; Sanbe, A.; Osinska, H.; Westfall, M.; Robinson, D.; Imahashi, K.; Murphy, E.; Robbins, J. Mitochondrial Dysfunction and Apoptosis Underlie the Pathogenic Process in Alpha-B-Crystallin Desmin-Related Cardiomyopathy. *Circulation* **2005**, *112*, 3451–3461.
18. Irwin, W. A.; Bergamin, N.; Sabatelli, P.; Reggiani, C.; Megighian, A.; Merlini, L.; Braghetta, P.; Columbaro, M.; Volpin, D.; Bressan, G. M.; *et al*. Mitochondrial Dysfunction and Apoptosis in Myopathic Mice with Collagen VI Deficiency. *Nat. Genet.* **2003**, *35*, 367–371.
19. Chandra, D.; Bratton, S. B.; Person, M. D.; Tian, Y.; Martin, A. G.; Ayres, M.; Fearnhead, H. O.; Gandhi, V.; Tang, D. G. Intracellular Nucleotides Act as Critical Prosurvival Factors by Binding to Cytochrome c and Inhibiting Apoptosome. *Cell* **2006**, *125*, 1333–1346.
20. Hao, Z.; Duncan, G. S.; Chang, C. C.; Elia, A.; Fang, M.; Wakeham, A.; Okada, H.; Calzascia, T.; Jang, Y.; You-Ten, A.; *et al*. Specific Ablation of the Apoptotic Functions of Cytochrome C Reveals a Differential Requirement for Cytochrome c and Apaf-1 in Apoptosis. *Cell* **2005**, *121*, 579–591.
21. Zhivotovsky, B.; Orrenius, S.; Brustugun, O.; Doskeland, S. Injected Cytochrome c Induces Apoptosis. *Nature* **1998**, *391*, 449–450.

22. Waterhouse, N. J.; Goldstein, J. C.; von Ahsen, O.; Schuler, M.; Newmeyer, D. D.; Green, D. R. Cytochrome C Maintains Mitochondrial Transmembrane Potential and ATP Generation after Outer Mitochondrial Membrane Permeabilization during the Apoptotic Process. *J. Cell Biol.* **2001**, *153*, 319–328.
23. Wang, J.; Li, M.; Shi, Z.; Li, N.; Gu, Z. Direct Electrochemistry of Cytochrome c at a Glassy Carbon Electrode Modified with Single-Wall Carbon Nanotubes. *Anal. Chem.* **2002**, *74*, 1993–1997.
24. Kam, N. W.; Dai, H. Carbon Nanotubes as Intracellular Protein Transporters: Generality and Biological Functionality. *J. Am. Chem. Soc.* **2005**, *127*, 6021–6026.
25. Zhou, F.; Wu, S.; Wu, B.; Chen, W. R.; Xing, D. Mitochondria-Targeting Single-Walled Carbon Nanotubes for Cancer Photothermal Therapy. *Small* **2011**, *7*, 2727–2735.
26. Kam, N. W.; Liu, Z.; Dai, H. Carbon Nanotubes as Intracellular Transporters for Proteins and DNA: An Investigation of the Uptake Mechanism and Pathway. *Angew. Chem., Int. Ed.* **2006**, *45*, 577–581.
27. Liu, Z.; Tabakman, S. M.; Chen, Z.; Dai, H. Preparation of Carbon Nanotube Bioconjugates for Biomedical Applications. *Nat. Protoc.* **2009**, *4*, 1372–1382.
28. Liu, Z.; Winters, M.; Holodniy, M.; Dai, H. siRNA Delivery into Human T Cells and Primary Cells with Carbon-Nanotube Transporters. *Angew. Chem., Int. Ed.* **2007**, *46*, 2023–2027.
29. Land, S. C.; Porterfield, D. M.; Sanger, R. H.; Smith, P. J. The Self-Referencing Oxygen-Selective Microelectrode: Detection of Transmembrane Oxygen Flux from Single Cells. *J. Exp. Biol.* **1999**, *202*, 211–218.
30. Blackburn, J. L.; McDonald, T. J.; Metzger, W. K.; Engtrakul, C.; Rumbles, G.; Heben, M. J. Protonation Effects on the Branching Ratio in Photoexcited Single-Walled Carbon Nanotube Dispersions. *Nano Lett.* **2008**, *8*, 1047–1054.
31. Mathur, A.; Hong, Y.; Kemp, B. K.; Barrientos, A. A.; Erusalimsky, J. D. Evaluation of Fluorescent Dyes for the Detection of Mitochondrial Membrane Potential Changes in Cultured Cardiomyocytes. *Cardiovasc. Res.* **2000**, *46*, 126–138.
32. Atlante, A.; Calissano, P.; Bobba, A.; Azzariti, A.; Marra, E.; Passarella, S. Cytochrome c Is Released from Mitochondria in a Reactive Oxygen Species (ROS)-Dependent Fashion and Can Operate as a ROS Scavenger and as a Respiratory Substrate in Cerebellar Neurons Undergoing Excitotoxic Death. *J. Biol. Chem.* **2000**, *275*, 37159–37166.
33. Skulachev, V. P. Cytochrome c in the Apoptotic and Antioxidant Cascades. *FEBS Lett.* **1998**, *423*, 275–280.
34. Dalmonte, M. E.; Forte, E.; Genova, M. L.; Giuffre, A.; Sarti, P.; Lenaz, G. Control of Respiration by Cytochrome c Oxidase in Intact Cells: Role of the Membrane Potential. *J. Biol. Chem.* **2009**, *284*, 32331–32335.
35. Margoliash, E.; Frohwirt, N. Spectrum of Horse-Heart Cytochrome c. *Biochem. J.* **1959**, *71*, 570–572.
36. Assfalg, M.; Bertini, I.; Dolfi, A.; Turano, P.; Mauk, A. G.; Rosell, F. I.; Gray, H. B. Structural Model for an Alkaline Form of Ferricytochrome *c*. *J. Am. Chem. Soc.* **2003**, *125*, 2913–2922.
37. Sivakolundu, S.; Mabrouk, P. Cytochrome *c* Structure and Redox Function in Mixed Solvents Are Determined by the Dielectric Constant. *J. Am. Chem. Soc.* **2000**, *122*, 1513–1521.
38. Kerr, L. E.; Birse-Archbold, J. L.; Short, D. M.; McGregor, A. L.; Heron, I.; Macdonald, D. C.; Thompson, J.; Carlson, G. J.; Kelly, J. S.; McCulloch, J.; *et al*. Nucleophosmin is a Novel Bax Chaperone that Regulates Apoptotic Cell Death. *Oncogene* **2007**, *26*, 2554–2562.
39. Yuan, J.; Gao, H.; Sui, J.; Duan, H.; Chen, W. N.; Ching, C. B. Cytotoxicity Evaluation of Oxidized Single-Walled Carbon Nanotubes and Graphene Oxide on Human Hepatoma HepG2 cells: An iTRAQ-Coupled 2D LC-MS/MS Proteome Analysis. *Toxicol. Sci.* **2012**, *126*, 149–161.
40. Kagan, V. E.; Tyurina, Y. Y.; Tyurin, V. A.; Konduru, N. V.; Potapovich, A. I.; Osipov, A. N.; Kisin, E. R.; Schwegler-Berry, D.; Mercer, R.; Castranova, V.; *et al*. Direct and Indirect Effects of Single Walled Carbon Nanotubes on RAW 264.7 Macrophages: Role of Iron. *Toxicol. Lett.* **2006**, *165*, 88–100.
41. Yang, Z.; Zhang, Y.; Yang, Y.; Sun, L.; Han, D.; Li, H.; Wang, C. Pharmacological and Toxicological Target Organelles and Safe Use of Single-Walled Carbon Nanotubes as Drug Carriers in Treating Alzheimer Disease. *Nanomed. Nanotechnol. Biol. Med.* **2010**, *6*, 427–441.
42. Azamian, B. R.; Davis, J. J.; Coleman, K. S.; Bagshaw, C. B.; Green, M. L. H. Bioelectrochemical Single-Walled Carbon Nanotubes. *J. Am. Chem. Soc.* **2002**, *124*, 12664–12665.
43. Heering, H. A.; Williams, K. A.; de Vries, S.; Dekker, C. Specific Vectorial Immobilization of Oligonucleotide-Modified Yeast Cytochrome c on Carbon Nanotubes. *ChemPhysChem* **2006**, *7*, 1705–1709.
44. Xu, W.; Charles, I. G.; Moncada, S. Nitric Oxide: Orchestrating Hypoxia Regulation through Mitochondrial Respiration and the Endoplasmic Reticulum Stress Response. *Cell Res.* **2005**, *15*, 63–65.
45. Smith, P. J. S.; Sanger, R. H.; Messerli, M. A. Principles, Development and Applications of Self-Referencing Electrochemical Microelectrodes to the Determination of Fluxes at Cell Membranes. In *Electrochemical Methods for Neuroscience*; Michael, A. C., Borland, L. M., Eds.; CRC Press: Boca Raton, FL, 2007; pp 373−405.